ESR Investigation of Radical Addition Reactions to 2-[(2,4,6-Tri-*tert*-Butyl)Phenyl]-1-Phosphaalkyne

Didier Gigmes,[†] Yves Berchadsky,[†] Jean-Pierre Finet,[†] Didier Siri,[‡] and Paul Tordo*[,†]

Laboratoire Structure et Réactivité des Espèces Paramagnétiques, case 521, CNRS UMR 6517 "Chimie, Biologie et Radicaux Libres", Universités d'Aix -Marseille I et III, Centre de Saint-Jérôme, Avenue Escadrille Normandie-Niemen, 13397 Marseille Cedex 20, France, and Laboratoire de Chimie Théorique et de Modélisation Moléculaire, case 521, CNRS UMR 6517 "Chimie, Biologie et Radicaux Libres", Universités d'Aix -Marseille I et III, Centre de Saint-Jérôme, Avenue Escadrille Normandie-Niemen, 13397 Marseille Cedex 20, France

Received: March 27, 2003; In Final Form: September 8, 2003

Radical additions of *tert*-butoxyl radical and alkylthiyl radicals to 2-[(2,4,6-tri-*tert*-butyl)phenyl]-1-phosphaalkyne have been investigated by ESR. The addition of oxygen or sulfur centered radical leads to an intermediate phosphavinyl σ-radical, which dimerizes to a 1,4-diphosphabutadiene, which undergoes a second radical addition to give a persistent π radical species. These species exhibit couplings with two different phosphorus nuclei and two different pairs of meta hydrogens. Our assignments were supported by ^{2}H labeling and ab initio calculations.

Introduction

In the early eighties, the first exceptions to the so-called "double bond rule",[1] which stipulated that stable (p-p) π multiple bonds should not be formed between, for example, phosphorus and elements of the first period, started to be observed. A number of kinetically stable species containing a P≡C bond is now known and among them, *tert*-butylphosphaacetylene has played a major role in the investigations of their chemical reactivity and their applications as building blocks in organometallic chemistry.[2] The reactivity of *tert*-butylphosphaacetylene has been more investigated than that of any other compound with a P≡C triple bond. In general, phosphaalkynes bearing tertiary alkyl substituents have a high thermal stability, but the steric hindrance of the bulky alkyl group does not affect significantly the reactivity. However, the behavior of the P≡C triple bond toward free radical addition remains still unknown. In the case of aryl-substituted phosphaalkynes, their reactivity has not been extensively studied, as only a small number of arylphosphaalkynes has been prepared. Among them, the unsubstituted phenylphosphaacetylene[3] is not stable enough for reactivity studies. The mesitylphosphaacetylene, recently prepared by Regitz et al.,[4] is more stable, but the presence of the three methyl substituents can interfere in the reaction of free radicals with the P≡C bond. The supermesitylphosphaacetylene **1**, 2-[(2,4,6-tri-*tert*-butyl)phenyl]-1-phosphaalkyne, can be easily prepared. Although it has a markedly reduced reactivity of the P/C triple bond because of the considerable shielding of the supermesityl group,[5] it can be an appropriate substrate for the study of the reactivity of the P≡C bond toward free radicals. In principle, addition of a free radical species to a phosphaalkyne such as **1** can follow two different paths: either addition through a phosphophilic attack or addition through a carbophilic attack. In the phosphophilic attack, formation of the bond between the incoming free radical species and the phosphorus atom will lead to phosphavinyl[6] σ radicals **2**. In the second type, the carbophilic attack will result in the formation of the phosphorus analogues, **3**, of iminyl radicals (Scheme 1). However, if we consider the addition of alkoxyl radicals, the strength of the P−O bond and the more important steric hindrance in the vicinity of the carbon atom than around the phosphorus atom of the triple bond of **1** will make a carbophilic attack very unlikely.

SCHEME 1

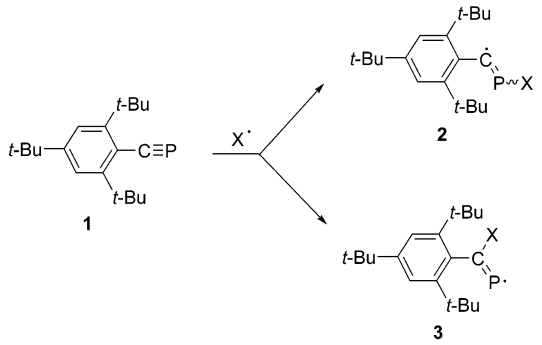

In this report, we describe our electron spin resonance (ESR) investigations of the addition on the triple bond of **1** of an alkoxyl radical (*t*-BuO$^\bullet$) and different alkythiyl radicals [RS$^\bullet$ (R = Me, *i*-Pr, *n*-Bu, *t*-Bu)].

Experimental Section

General. ^{1}H NMR spectra were recorded at 100 and 400 MHz in C_6D_6 using TMS as internal reference. ^{31}P NMR (40.53 MHz) was taken in C_6D_6 using 85% H_3PO_4 as an internal standard with broadband ^{1}H decoupling. ^{13}C NMR spectral measurements were performed at 100.6 MHz using C_6D_6. δ values are given in ppm and J values in hertz. Elemental analyses were determined at the University of Aix-Marseille III. ESR spectra were recorded using a Bruker ESP 300 spectrometer at 9.5 GHz (X-band) employing 100 kHz field

* Corresponding author. E-mail: ptordo@srepir1.univ-mrs.fr.
[†] Laboratoire Structure et Réactivité des Espèces Paramagnétiques.
[‡] Laboratoire de Chimie Théorique et de Modélisation Moléculaire.

10.1021/jp034784p CCC: $25.00
Published on Web 10/18/2003

TABLE 1: Experimental ESR Parameters of the Spectrum A Displayed in Figure 1

a_1/mT	a_2/mT	ΔHpp/mT[a]	g
0.81	2.29	0.305	2.0024

[a] ΔHpp for the main four lines of the spectrum.

modulation. ESR spectra were simulated using the ESR software developed by D. Duling from the laboratory of Molecular Biophysics, NIEHS (this software is available via the Internet at http://EPR.niehs.nih.gov).[13] Samples were heated via a Bruker variable temperature unit ER 4111 VT. UV photolysis was performed by a 1000 W xenon−mercury Oriel lamp. Melting points were measured on a Büchi capillary apparatus and are uncorrected. All the reagents were purchased from Aldrich.

The phosphaalkynes **1**, **5**, and **10** were prepared by the procedure described by Romanenko et al.[14] 2-[(2,4,6-Tri-*tert*-butyl-3,5-dideutero)phenyl]-1-phosphaalkyne **5** was prepared using benzene-d_6 as starting material. In the synthesis of 2-[(2,4,6-tri-*tert*-butyl-d_9)phenyl]-1-phosphaalkyne **10**, 2-chloro-2-methylpropane-d_9 was used for the introduction of the three perdeuterated *tert*-butyl groups on benzene.[15] *tert*-Butyl hyponitrite was prepared according to the procedure described by Kiefer and Traylor.[16]

2-[(2,4,6-Tri-*tert*-butyl)phenyl]-1-phosphaalkyne 1. M.p. 124 °C; ^{31}P NMR (40.53 MHz, C_6D_6): δ 33.2; ^{1}H NMR (100 MHz, C_6D_6): δ 7.43 (s, 2H), 1.72 (s, 18H), 1.23 (s, 9H); ^{13}C NMR (100.6 Mz, C_6D_6): δ 169.28 (C═P, d, $^1J_{CP}$ = 53.5); 157.28 (C2, d, $^3J_{CP}$ = 5.8); 151.63 (C4, d, $^5J_{CP}$ = 5.9); 125.20 (C1, d, $^2J_{CP}$ = 22); 121.33 (s, C3); 37.22 (s, *o*-*C*Me$_3$); 35.45 (s, *p*-*C*Me$_3$); 31.38 (s, *p*-C*Me*$_3$); 31.18 (s, *o*-C*Me*$_3$). Calcd for $C_{19}H_{29}P$ (288 g mol^{-1}): C, 79.13; H, 10.14. Found C, 79.12; H, 10.12%.

2-[(2,4,6-Tri-*tert*-butyl-3,5-di-deutero)phenyl]-1-phosphaalkyne 5. M.p. 124 °C. ^{31}P NMR (40.53 MHz, C_6D_6): δ 32; ^{1}H NMR (100 MHz, C_6D_6): δ 1.76 (s, 18H), 1.25 (s, 9H). Calcd for $C_{19}H_{27}D_2P$ (290 g mol^{-1}) C, 78.57; H 9.57. Found C 78.60; 9.54%.

2-[(2,4,6-Tri-*tert*-butyl-d_9)phenyl]-1-phosphaalkyne 10. M.p. 126 °C. ^{31}P NMR (40.53 MHz): δ 32.3. ^{13}C NMR (100.6 MHz, C_6D_6): δ 169.33 (C═P, d, $^1J_{CP}$ = 52); 157.31 (d, C2, $^3J_{CP}$ = 6); 151.69 (d, C4, $^5J_{CP}$ = 5); 125.4 (d, C1, $^2J_{CP}$ = 22); 121.30 (s, C3); 38.01 (s, *o*-*C*Me$_3$); 36.56 (s, *p*-*C*Me$_3$); 29.4−31.2 (m, C*Me*$_3$).

Results and Discussion

a. Addition of *tert*-BuO• Radical. The alkoxyl radical (*t*-BuO•) was generated in situ either by thermolysis of *tert*-butylhyponitrite or by photolysis of di-*tert*-butylperoxide. When a *tert*-butylbenzene solution (10^{-3} M) of 2-[(2,4,6-tri-*tert*-butyl)-phenyl]-1-phosphaalkyne **1** was heated at 303 K in the presence of *tert*-butylhyponitrite or when a cyclopropane solution (10^{-3} M) of **1** was photolyzed in the presence of di-*tert*-butylperoxide, an intense ESR signal **A** composed of a main doublet of doublet (a_1 = 0.81 mT and a_2 = 2.29 mT, Table 1) with further small hyperfine splittings was observed (Figure 1). The signal was persistent in the temperature range 153 K to 313 K and lasted for a few hours after the generation of the *tert*-butoxyl radical was stopped.

Signal **A** was characterized by a value of the Landé factor (g = 2.0024) close to that of carbon centered radicals;[7] all its ESR characteristics are not compatible with a radical adduct like **3** (X = *t*-BuO), which should exhibit a larger phosphorus coupling and a larger g value.

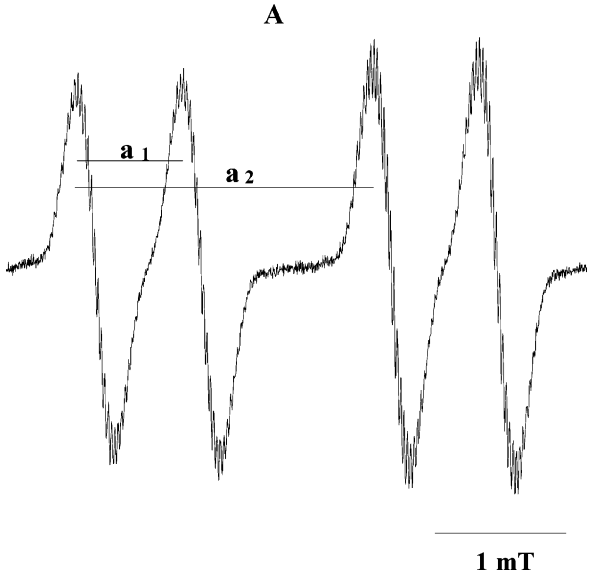

Figure 1. ESR spectrum observed when heating at 303 K a degassed solution of **1** and *tert*-butyl hyponitrite in *tert*-butyl benzene.

SCHEME 2

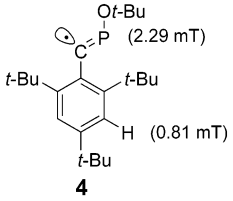

SCHEME 3

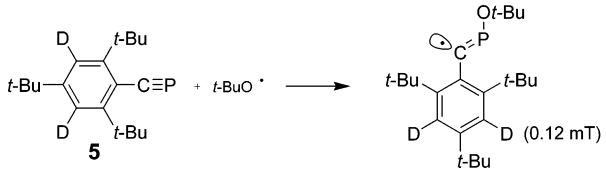

The more probable addition of the *tert*-butoxyl radical on the phosphorus atom of **1** leads to the radical adduct **4** which, due to steric crowding, is likely to exist only as the E isomer. In such a case, the large coupling constant observed in spectrum **A** could be assigned to the phosphorus atom while the smaller one should originate from a long-range W coupling with a meta hydrogen[8] of the aromatic ring (Scheme 2).

However, for a structure such as **4**, the magnitude of this hypothetical long-range W coupling is rather large.[8,9] Moreover, the high persistency of signal **A** seems unusual for this kind of radicals.[6]

To find out if spectrum **A** could be nevertheless attributed to the radical adduct **4**, we decided to prepare the meta dideuterated phosphalkyne **5**. Indeed, substitution of a deuterium atom to the hydrogen atom in the meta positions should result, after addition of *t*-BuO• on the P≡C bond, in the observation of a doublet of triplet resulting from the coupling with one deuterium atom with a hyperfine splitting constant close to 0.12 mT (Scheme 3).

When a solution of **5** in *tert*-butylbenzene (10^{-3} M) was heated in the presence of *tert*-butylhyponitrite in the ESR cavity, the observed spectrum was again composed of a doublet of doublet with ESR parameters (Table 2) identical to those obtained with **1**, but the small long-range hyperfine splittings were not resolved (spectrum B, Figure 2). This result indicated

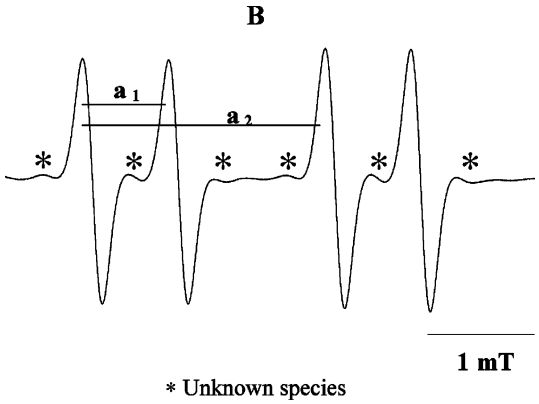

Figure 2. ESR spectrum observed when heating at 303 K a degassed solution of **5** and *tert*-butyl hyponitrite in *tert*-butyl benzene.

TABLE 2: Experimental ESR Parameters of the Spectrum B Displayed in Figure 2

a_1/mT	a_2/mT	ΔHpp/mT	g
0.815	2.289	0.186	2.0024

that the ESR signal **A** is not consistent with the radical structure **4**. On the other hand, the weaker line width (0.186 mT) observed in spectrum **B** compared to that of a main line of signal **A** (0.305 mT) proves that the hydrogen atoms in the meta position in the radical adduct derived from **1** participate only in the broadening of the line width. Thus, it can be concluded that the weakest coupling constant (a_1) of spectrum **A** does not originate from one of the meta hydrogen atoms of the radical **4**.

If we look at the fate of a species such as **4**, two main possible evolutions can be considered. Hydrogen abstraction from one of the neighboring *tert*-butyl groups, followed by addition of the newly formed radical center to the C═P double bond could lead to the six-membered ring heterocyclic free radical **7** (Scheme 4). On the other hand, the dimerization of the very reactive vinyl type radical **4** to form the neutral diphosphabutadiene derivative **8** should also be considered. Subsequent addition of *t*-BuO$^\bullet$ to **8** would generate the radical **9** (Scheme 4).

The very small hyperfine splittings, observed in the case of spectrum **A** (Figure 1), are likely to arise from the hydrogen atoms of either the *tert*-butyl groups or the *tert*-butoxyl groups. These splittings could mask other coupling constants that could help to identify the radical species obtained upon reaction of *t*-BuO$^\bullet$ with **1**. In a further attempt to elucidate the structure of the radical giving spectrum **A**, the reaction of the phosphaalkyne **10**, containing perdeuterated *tert*-butyl groups, with *tert*-butylhyponitrite was investigated by ESR.

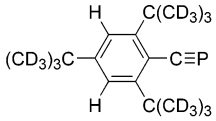

10

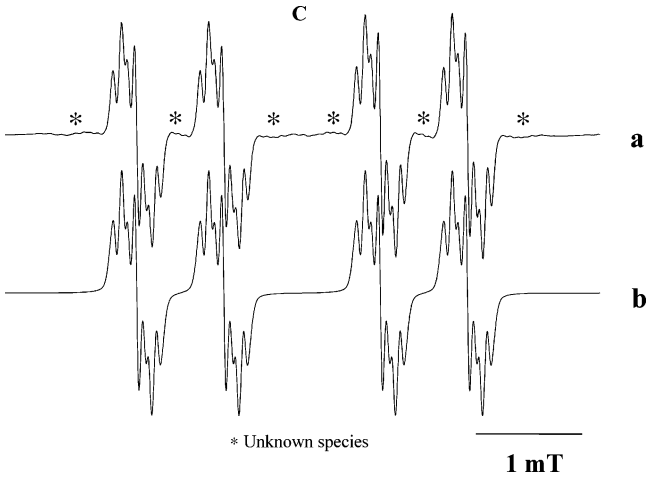

Figure 3. ESR spectrum observed when heating at 303 K a degassed solution of **10** and *tert*-butyl hyponitrite in *tert*-butyl benzene. (a) experimental (b) simulated.

When a degassed solution of the phosphaalkyne **10** and *tert*-butylhyponitrite in *tert*-butylbenzene was heated at 303 K, the observed ESR spectrum (Figure 3) was again composed of a main doublet of doublet with the same coupling constants (a_1, a_2) and *g* factor as those observed in the ESR experiments carried out either with **1** or with **5**. However, in this case, further smaller couplings were resolved. The permanence of a main doublet of doublet on the ESR spectra ($a_1 = 2.3$ mT, $a_2 = 0.8$ mT) observed when the radical *t*-BuO$^\bullet$ was added to **1**, **5**, or **10**, clearly indicates that this common spectral pattern arises from the coupling with two phosphorus nuclei. Then, we assigned the spectrum **C** (Figure 3) to the dimeric species **11** obtained as shown on Scheme 4 (compound **9**). This ESR spectrum was nicely simulated (Figure 3) by considering one large coupling with the phosphorus atom P_2, a small one with

SCHEME 4

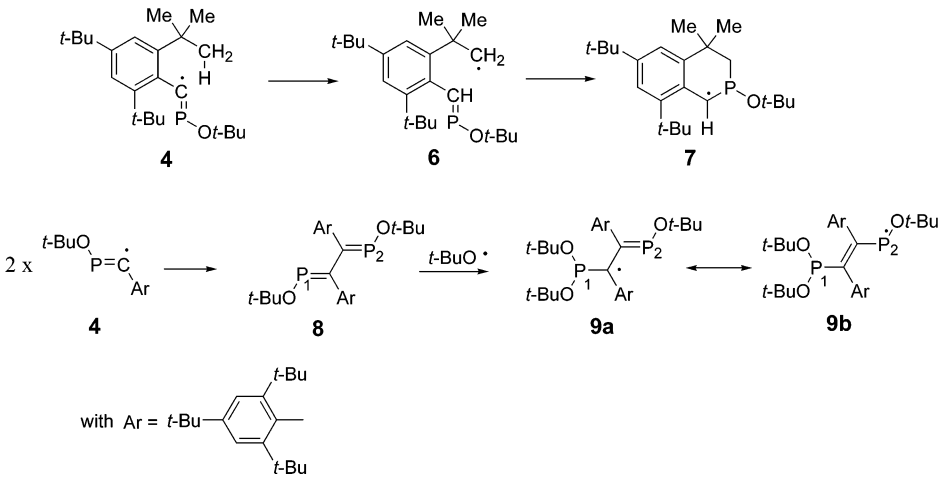

TABLE 3: Hyperfine Splitting Constants (mT) for Radical 11 Obtained from the Simulated Spectrum

a_{P1}	a_{P2}	$2xa_{H(m)}$	$2xa_{H(m)}$
0.821	2.30	0.125	0.075

TABLE 4: Calculated (DFT) and Experimental Hyperfine Couplings (mT) and Total Atomic Spin Densities for Radical 12

atoms	P_1	P_2	$C(P_1)$	$C(P_2)$
experimental hyperfine coupling constant	0.821	2.30		
DFT calculated hyperfine coupling constant	0.16	5.35	0.89	−0.81
total atomic spin density (a.u.)	−0.008	0.783	0.231	−0.101

the phosphorus atom P_1, and the coupling with two pairs of meta hydrogens (Table 3).

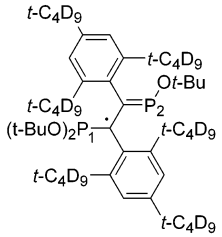

11

To rationalize these hypotheses, we have performed ab initio calculations at the UB3LYP/TZVP//UB3LYP/3-21G level with the Gaussian 98 package.[10] Indeed this functional and this basis set have been already used to calculate hyperfine splitting constants on phosphorylated compounds.[11] Because of the large size of the molecule **9**, calculations were performed on the model radical **12** in which all the *t*-Bu groups were replaced by methyl groups and the para *t*-Bu groups were not considered.

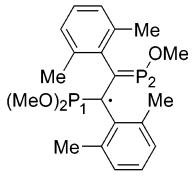

12

Compared to molecule **9**, these structural simplifications should lower the steric hindrance. Therefore the conformation will be modified, but the electronic distributions should have the same trends. The calculated total atomic spin densities and calculated hyperfine couplings are displayed in Table 4.

Although the calculated (DFT) and experimental hyperfine coupling constants are not very close, they exhibit the same tendency. As observed on the experimental spectrum, the calculations led to a large ^{31}P for one phosphorus and a smaller one for the other phosphorus nucleus.

SCHEME 5. Mesomeric Forms for Compound 12

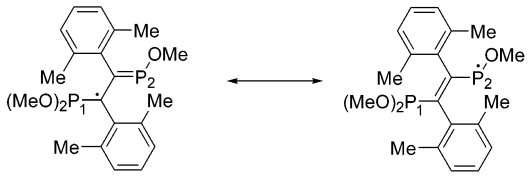

12a **12b**

TABLE 5: Hyperfine Splitting Constants (mT) for Radical 9 Obtained from the Simulated Spectrum

a_{P1}	a_{P2}	$2xa_{H(m)}$	$2xa_{H(m)}$	$18xa_{H(2\ o-tBu)}$	$9xa_{H(p-tBu)}$
0.821	2.30	0.125	0.075	0.029	0.024

TABLE 6: Hyperfine Splitting Constants (mT) for Radical 13 Obtained from the Simulated Spectrum

a_{P1}	a_{P2}	$2xa_{D(m)}$	$2xa_{D(m)}$	$18xa_{H(2\ o-tBu)}$	$9xa_{H(p-tBu)}$
0.82	2.29	0.019	0.012	0.029	0.024

From the data of Table 4, it appears that the spin density is essentially distributed between the four atoms [P_1, P_2, $C(P_1)$, $C(P_2)$] with a major contribution for the P_2 and $C(P_1)$ atoms. This means that radical **12** can be represented by a hybrid of the two mesomeric forms **12a** and **12b** (Scheme 5). Indeed, if the reaction of *t*-BuO$^\bullet$ with **1**, **5**, or **10** leads to a type of radical like **9**, a large coupling constant value with P_2 and a small one with P_1 will be expected to be observed by ESR.

Thus, the spectrum **A** resulting from the interaction of *t*-BuO$^\bullet$ with the phosphaalkyne **1** can be attributed to the radical species **9** (Scheme 4). Due to the steric hindrance of the *tert*-butoxy groups, only the E isomer was observed by ESR. Finally, the experimental spectrum A has been satisfactorily simulated (Figure 4) by considering the couplings with two phosphorus atoms P_1 and P_2, two pairs of hydrogen in the meta positions of the two aromatic rings, eighteen hydrogens of the two ortho *tert*-butyl groups, and nine hydrogens of the para *tert*-butyl group of only one aromatic ring (Table 5). The difference observed between the two pairs of meta hydrogens is in agreement with the spin density distribution.

The resolution observed on the ESR spectra obtained after reaction of *t*-BuO$^\bullet$ radical with **1** or **5** was different (compare Figures 1 and 2). The lack of resolution in the case of **5** could be attributed to the presence of the deuterium atoms in meta position of the aromatic ring. To check this hypothesis we performed the simulation of the experimental spectrum displayed in Figure 2 by using the values listed in Table 5. As shown in Figure 5, a very good agreement was obtained between the experimental and simulated spectrum (Figure 5, Table 6). Therefore, the spectrum displayed on Figure 5 could be assigned

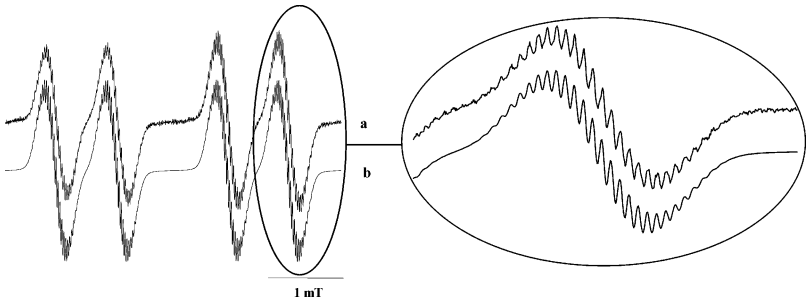

Figure 4. ESR spectrum observed when heating at 303 K a degassed solution of **1** and *tert*-butyl hyponitrite in *tert*-butyl benzene. (a) experimental (b) simulated.

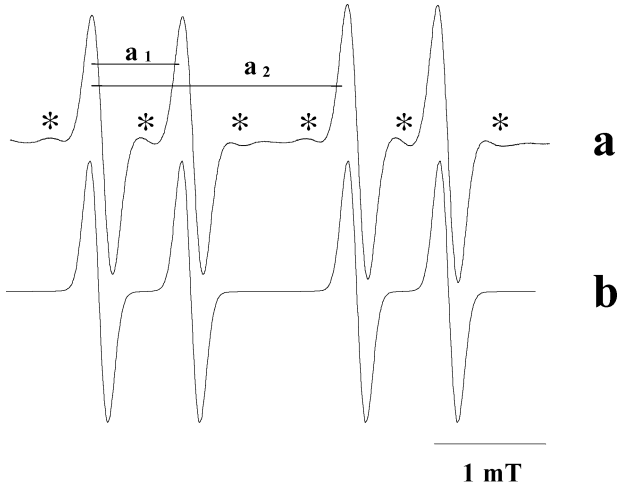

Figure 5. ESR spectrum observed when heating at 303 K a degassed solution of **5** and *tert*-butyl hyponitrite in *tert*-butyl benzene. (a) experimental (b) simulated.

to the radical structure **13**, and the blurring attributed to the presence of deuterium atoms.

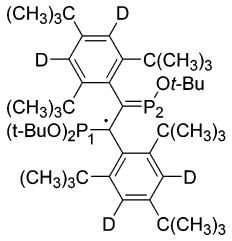

b. Addition of Alkylthiyl Radicals RS•. When a degassed *tert*-butylbenzene solution of the phosphaalkynes **1** or **10** in the presence of di-*tert*-butylsulfide was photolyzed inside the ESR spectrometer cavity, we observed changes in the patterns of the corresponding ESR spectra (spectrum **D** with **1** and spectrum **E** with **10**) similar to those observed when the experiments were performed with *tert*-butylhyponitrite (Figure 6). However, when **1** or **10** was allowed to react with *tert*-butylthiyl radical, the ESR signals contained eight lines, while only four main lines were observed when **1** or **10** was reacted with *t*-BuO•. According to our previous results, we assigned this eight-line signal to the superimposition of the spectra of two isomer radicals **14** and **15** with a major contribution from the *E* isomer **14**.

TABLE 7: ESR Parameters for 14 and 15 with R = *t*-Bu Determined from the Simulated Spectrum

radical[a]	a_{P1}/mT	a_{P2}/mT	$2xa_{H(m)}$/mT	$2xa_{H(m)}$/mT	%	g
14 (×)	0.786	2.253	0.119	0.078	70	2.0026
15 (●)	0.627	5.151	0.103	0.103	30	2.0029

[a] (×) corresponds to the four lines of the major signal observed in the ESR spectrum (Figure 5) and (●) to the minor isomer.

TABLE 8: Calculated (DFT) Hyperfine Couplings (mT) and Total Atomic Spin Densities for Radical 16

radicals	$^{31}P_1$ coupling/mT	$^{31}P_2$ coupling/mT
16 (*E*)	1.24	4.13
16 (*Z*)	1.22	4.41

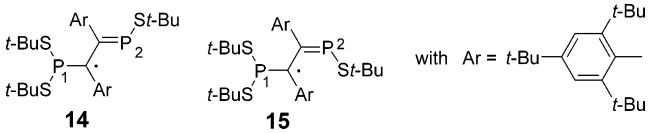

These results suggest that *t*-BuO• and *t*-BuS• radicals react with phosphaalkyne **1** under similar chemical pathways. However, the P−S bond being longer than the P−O bond, the lower steric hindrance of the *t*-BuS group permits the observation of the *Z* isomer. The experimental spectra were satisfactorily simulated with the hyperfine splitting constants collected in Table 7.

With the aim of rationalizing the difference observed on the ^{31}P2 hyperfine splitting constants between the isomers *E* and *Z*, we have carried out DFT calculations (UB3LYP/TZVP// UB3LYP/3-21G) on the model molecule **16**, and the results are shown in Table 8. As experimentally observed, the DFT calculated (Table 8) couplings show also a difference for the $^{31}P_2$ splitting between the isomers *E* and *Z*. The $^{31}P_2$ coupling calculated for the *Z* isomer is larger than the one obtained for the *E* isomer, but in an order of magnitude smaller than those

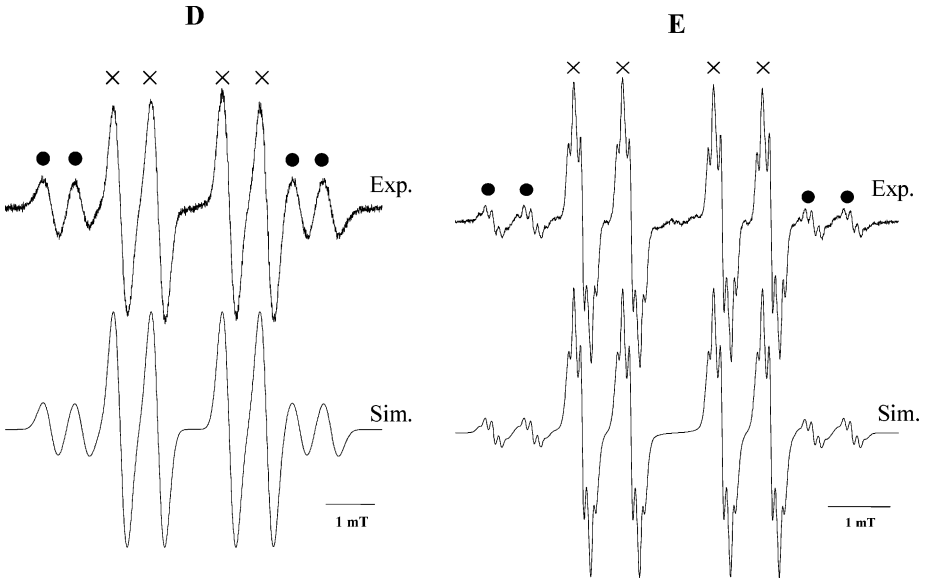

Figure 6. Experimental (Exp.) and simulated (Sim.) ESR spectra observed during the photolyzing of *tert*-butyl disulfide at 298 K in a degassed *tert*-butyl benzene solution of **1** (spectrum D) and **10** (spectrum E).

TABLE 9: Experimental Hyperfine Splitting Constants for the Reaction of Alkylthiyl Radicals on Phosphaalkyne 1

thiyl radical	isomer	a_{P1}/mT	a_{P2}/mT	g
t-BuS•	E	0.79	2.25	2.0026
	Z	0.63	5.15	2.0029
MeS•	E	0.72	2.22	2.0026
	Z	0.62	5.10	2.0032
i-PrS•	E	0.80	2.22	2.0028
	Z	0.70	5.20	2.0032
n-BuS•	E	0.77	2.22	2.0028
	Z	0.65	5.12	2.0032

experimentally observed. The discrepancy between the calculated and experimental values is probably due to the model molecule used to perform the calculations. Compared to the model radical **16**, the radical species **14** and **15** exhibit a higher steric hindrance. Molecular mechanic calculations[12] performed on **14** and **16** show that the aromatic rings are planar for **16** and sligthly puckered for **14**. Moreover, the bond length between the aryl group and the carbon atom bound are also different (1.48 vs 1.51 for **16** and **14**, respectively). These structural modifications should affect significantly the electronic properties of the aromatic ring and therefore the value of the hyperfine splitting constants.

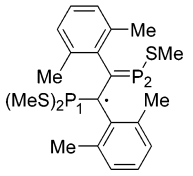

16 (*E*)

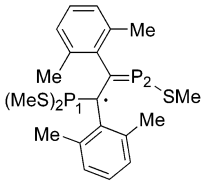

16 (*Z*)

ESR investigations of radical addition onto 2-[2,4,6-tri-*tert*-butyl)phenyl]-1-phosphaalkyne **1** were extended to other less hindered alkylthiyl radicals (Table 9). In each case, the ESR parameters and isomer ratios were similar to those obtained in the reaction with *t*-BuS•. This result indicates that the nature of the alkylthiyl radical does not affect the formation of the radical species **14** and **15**.

Conclusion

According to our ESR results, the vinyl type radical formed upon addition of *t*-BuO• and RS• radicals to 2-[(2,4,6-tri-*tert*-butyl)phenyl]-1-phosphaalkyne **1** dimerizes rapidly to form a phosphabutadiene. Subsequent addition of *t*-BuO• and RS• to the phosphabutadiene moiety yields a persistent π radical exhibiting couplings with two different phosphorus nuclei and two different pairs of meta hydrogens. Our assignments were supported by ^{2}H labeling and ab initio calculations.

Acknowledgment. We thank the Université de Provence and CNRS for financial support.

References and Notes

(1) Nixon, J. F. *Chem. Ind.* **1993**, *11*, 404−407. Hoogenboom, B. E. *J. Chem. Educ.* **1998**, *75*, 596−603.

(2) (a) Yoshifuji, M. *J. Organomet. Chem.* **2000**, *611*, 210−216. (b) Regitz, M. *Chem. Rev.* **1990**, *90*, 191−213. (c) Regitz, M.; Binger, P. *Angew. Chem.* **1988**, *100*, 1541−1565; *Angew. Chem., Int. Ed. Engl.* **1988**, *27*, 1484−1508. (d) Regitz, M. In *Multiple Bonds and Low Coordination in Phosphorus Chemistry*; Regitz, M., Scherer, O. J., Eds.; Thieme: Stuttgart, 1990; p 77. (e) Regitz, M.; Hoffmann, A.; Bergsträsser, U. In *Modern Acetylene Chemistry*; Stang, P. J., Diederich, F., Eds.; VCH: Weinheim, 1995; p 173.

(3) Appel, R.; Maier, G.; Reisenauer, H.-P.; Westerhaus, A. *Angew. Chem.* **1981**, *93*, 215; *Angew. Chem., Int. Ed. Engl.* **1981**, *20*, 197.

(4) Mack, A.; Pierron, E.; Allspach, T.; Bergsträsser, U.; Regitz M. *Synthesis* **1998**, 1305−1313.

(5) Märkl, G.; Sejpka, H. *Tetrahedron Lett.* **1986**, *27*, 171−174.

(6) Alberti, A.; Benaglia, M.; D'Angelantonio, M.; Emmi, S. S.; Guerra, M.; Hudson, A.; Macciantelli, D.; Paolucci, F.; Roffia, S. *J. Chem. Soc., Perkin Trans. 2* **1999**, 309−324.

(7) Landolt-Börnstein; *Magnetic Properties of Free Radicals*; New Series, Vol II/1, II/9b, II/17b; Fischer, H., Ed.; Springer: Berlin, 1965−1986.

(8) Gronchi, G. *Doctorat Sciences Université Aix-Marseille 3*, 1984.

(9) Krusic, P. J.; Rettig, T. A. *J. Am. Chem. Soc.* **1970**, *92*, 722−724.

(10) Frisch, M. J.; Trucks, G. W.; Schlegel, H. B.; Scuseria, G. E.; Robb, M. A.; Cheeseman, J. R.; Zakrzewski, V. G.; Montgomery, J. A.; Stratmann, R. E., Jr.; Burant, J. C.; Dapprich, S.; Millam, J. M.; Daniels, A. D.; Kudin, K. N.; Strain, M. C.; Farkas, O.; Tomasi, J.; Barone, V.; Cossi, M.; Cammi, R.; Mennucci, B.; Pomelli, C.; Adamo, C.; Clifford, S.; Ochterski, J.; Petersson, G. A.; Ayala, P. Y.; Cui, Q.; Morokuma, K.; Malick, D. K.; Rabuck, A. D.; Raghavachari, K.; Foresman, J. B.; Cioslowski, J.; Ortiz, J. V.; Baboul, A. G.; Stefanov, B. B.; Liu, G.; Liashenko, A.; Piskorz, P.; Komaromi, I.; Gomperts, R.; Martin, R. L.; Fox, D. J.; Keith, T.; Al-Laham, M. A.; Peng, C. Y.; Nanayakkara, A.; Gonzalez, C.; Challacombe, M.; Gill, P. M. W.; Johnson, B.; Chen, W.; Wong, M. W.; Andres, J. L.; Gonzalez, C.; Head- Gordon, M.; Replogle, E. S.; Pople, J. A. *Gaussian 98*, revision A.7; Gaussian, Inc.: Pittsburgh, PA, 1998.

(11) Rosa, P.; Gouverd, C.; Bernadinelli, G.; Berclaz, T.; Geoffroy, M. *J. Phys. Chem. A* **2003**, *107*, 4883−4892. Nguyen, M. T.; Creve, S.; Eriksson, L. A.; Vanquickenborne, L. G. *Mol. Phys.* **1997**, *91*, 537. Koch, W.; Holthausen, M. C. *A Chemist's Guide to Density Functional Theory*; Wiley-VCH: Verlag GmbH, Weinheim, 2001; 212−215. Godbout, N.; Salahub, D. R.; Andzelm, J.; Wimmer, E. *Can. J. Chem.* **1992**, *70*, 560.

(12) Pepe, G.; Siri, D. *Stud. Phys. Theor. Chem.* **1990**, *71*, 93−101.

(13) Duling, D. R. *J. Magn. Reson., Ser. B* **1994**, *104*, 105−110.

(14) Romanenko, V. D.; Sanchez, M.; Sarina, T. V.; Mazières, M.-R.; Wolf, R. *Tetrahedron Lett.* **1992**, *33*, 2981−2982. Heller, C.; McConnell, H. M. *J. Chem. Phys.* **1960**, *32*, 1535−1539.

(15) Baas, J. M. A.; Van Bekkum, H.; Hoefnagel, M. A.; Wepster, B. M. *Recl. Trav. Chim. Pays-Bas* **1969**, *88*, 1110−1114.

(16) Kiefer, H.; Traylor, T. G. *Tetrahedron Lett.* **1966**, 6163−6168.